Study on Wear Properties of the Flow Parts in a Centrifugal Pump Based on EDEM?Fluent Coupling

Authors:

Si Huang, Jiaxing Huang, Jiawei Guo, Yushi Mo

Date Submitted: 2019-09-13

Keywords: numerical simulation, wear, solid–liquid two-phase flow, EDEM–Fluent coupling, centrifugal pump

Abstract:

By using EDEM?Fluent codes and coupling the continuous fluid medium with a solid particle discrete element, the solid?liquid two-phase flow field in a centrifugal pump was simulated under the same inlet conditions of the particle volume fraction and three flow conditions of 0.7Qd, 1.0Qd and 1.3Qd. By introducing the Archard wear model, the wear was calculated, and the wear law was obtained for the pump flow parts such as the leading edge of the impeller blade, blade tip, blade pressure side, blade suction side, impeller shroud, hub and volute. The results demonstrate that the wear of volute is about 70% of the total wear of pump. The wear in the impeller mainly occurs in the blade leading edge, the junction of the hub and the trailing part of the blade pressure side, and the junction of the shroud and the rear part of the blade suction side. Under lower flow conditions, the wear in the impeller shroud is relatively considerable. As the flow rate increases, the wear in the blade pressure side and the hub increases significantly.

Record Type: Published Article

Submitted To: LAPSE (Living Archive for Process Systems Engineering)

Citation (overall record, always the latest version): LAPSE:2019.1010
Citation (this specific file, latest version): LAPSE:2019.1010-1
Citation (this specific file, this version): LAPSE:2019.1010-1v1

DOI of Published Version: https://doi.org/10.3390/pr7070431

processes

MDPI

Article

Study on Wear Properties of the Flow Parts in a Centrifugal Pump Based on EDEM–Fluent Coupling

Si Huang [1,*], Jiaxing Huang [1], Jiawei Guo [1] and Yushi Mo [2]

[1] School of Mechanical and Automotive Engineering, South China University of Technology, Guangzhou 510640, China
[2] Kenflo Pumps Co. Ltd., Foshan 528000, China
* Correspondence: huangsi@scut.edu.cn; Tel.:+86-137-2520-0827

Received: 21 June 2019; Accepted: 4 July 2019; Published: 9 July 2019

Abstract: By using EDEM–Fluent codes and coupling the continuous fluid medium with a solid particle discrete element, the solid–liquid two-phase flow field in a centrifugal pump was simulated under the same inlet conditions of the particle volume fraction and three flow conditions of $0.7Q_d$, $1.0Q_d$ and $1.3Q_d$. By introducing the Archard wear model, the wear was calculated, and the wear law was obtained for the pump flow parts such as the leading edge of the impeller blade, blade tip, blade pressure side, blade suction side, impeller shroud, hub and volute. The results demonstrate that the wear of volute is about 70% of the total wear of pump. The wear in the impeller mainly occurs in the blade leading edge, the junction of the hub and the trailing part of the blade pressure side, and the junction of the shroud and the rear part of the blade suction side. Under lower flow conditions, the wear in the impeller shroud is relatively considerable. As the flow rate increases, the wear in the blade pressure side and the hub increases significantly.

Keywords: centrifugal pump; EDEM–Fluent coupling; solid–liquid two-phase flow; wear; numerical simulation

1. Introduction

Centrifugal pumps are used to transport solid–liquid two-phase media for many occasions. The wear produced by sand particles directly affects the hydraulic performance and operational life of the pump. In recent years, many investigations into the solid–liquid two-phase flow field in the centrifugal pump have been undertaken [1–5]. Also, researchers have conducted numerous investigations on the erosion wear of centrifugal pumps by means of different numerical and experimental methods [6–19]. For example, Noon et al. [6] simulated the erosion wear of the volute and found that the tongue and downstream of the volute are the most severe regions of wear. Shen et al. [7] studied the effect of particle parameters on erosion wear in the pump, and found that an increase in particle velocity seriously aggravates erosion wear. Lei et al. [10] measured the wear of the impeller blade under different flow conditions, stating that the wear on the blade suction side is more severe than the pressure side under lower flow conditions, and the pressure side wear is more severe under higher flow conditions. Luo et al. [13] experimentally studied the erosion wear of the impeller blade and reported that the erosion wear is more severe in the blade leading edge, the pressure side and the rear part of the suction side. Roco [14] conducted a paint wear experiment to investigate the wear in the pump under different pump geometries and sediment concentrations. He observed the average wear of the volute is highest with all components. Ahmad et al. [15] developed a numerical software to research the wear in the pump and then compared the results of the paint wear experiment. They proposed that the blade leading edge wears most severely and the blade pressure side erodes faster than the suction side. Azimian et al. [16] set up an erosion tester to study the slurry erosion under different

flow conditions, finding an increasing trend of erosion when increasing the flow rate. Tao et al. [17] designed a wear test rig to determine the abrasion of impellers, finding that the areas with more severe abrasion are located at the blade leading edge and the junction between the blade pressure side and the hub. However, the wear law of solid–liquid two-phase flow centrifugal pumps obtained from the research above is essentially qualitative, lacking the detailed quantitative wear law of each flow passage part in the pump.

In this paper, solid–liquid two-phase flow in the pump under different flow conditions was performed by coupling the continuous fluid medium with the solid particle discrete element in the EDEM (a Discrete Element Method software for bulk material simulation.) and Fluent code. The wear properties of all the flow parts in the centrifugal pump were carried out by introducing the wear model, which could provide the theoretical foundation for improving the operating efficiency and reliability of the solid–liquid two-phase flow centrifugal pump.

2. Models and Methods

2.1. EDEM–Fluent Coupling Method

The EDEM–Fluent coupling process is illustrated in Figure 1. The discrete element method (DEM) and computational fluid dynamics (CFD) are used to describe particle motion and fluid flow respectively, and the mutual transfer of momentum and energy is further carried out through the application programming interface (API) [19,20]. This method combines the advantages of DEM and CFD to simulate particle motion and interaction with the flow field more accurately.

In the simulation, liquid in the pump was considered as the continuous phase, and the solid particles were considered as the discrete phase. The transient flow field is initially simulated using Fluent software (ANSYS Inc., Canonsburg, PA, USA) with solutions of the transient Reynolds averaged Navier–Stokes (RANS) equation and the standard k-epsilon turbulence model. The calculation result is subsequently transferred to the EDEM software (DEM Solutions Ltd., Edinburgh, UK) to solve the force, velocity and collision characteristics of particles according to Newton's second law, while taking into account the particle size, shape and material properties.

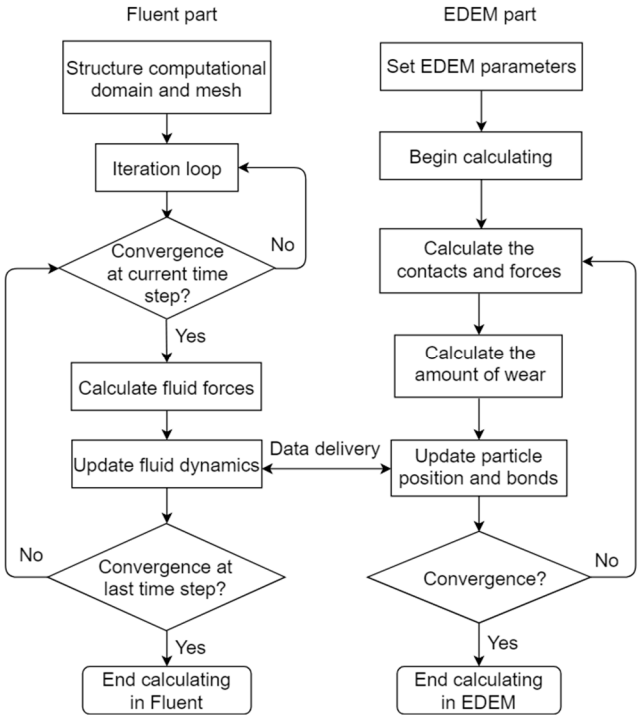

Figure 1. EDEM–Fluent coupling process.

2.2. Wear Model

The common wear models related to solid particles include the Finnie model [21], the Tabakoff model [22], and the Archard model [23]. The Archard wear model was built in the EDEM software, represented by the wear volume, W, and the formula is presented below.

$$W = \frac{K}{H} F_n L \tag{1}$$

where K is the wear coefficient, H is the material surface hardness, F_n is the normal load, and L is the friction distance. In EDEM, the wear volume is also expressed as the wear per unit flow area h:

$$h = \frac{W}{A} \tag{2}$$

where A is the contact area between the solid particles and the flow part.

2.3. Computational Model and Meshing

The commonly used centrifugal pump of type IS (a type of single-stage single-suction centrifugal pump) was chosen for this study, as shown in Figure 2. The design parameters are: the capacity Q_d = 99 m^3/h, the head H_d = 13.6 m, and the speed n = 1450 rpm. The direction of gravitational acceleration (g = 9.81 m/s^2) was opposite to the flow entering the pump inlet. For the purpose of investigating the effect of cell numbers on the calculation results, a grid independence test was conducted on different cell numbers. As can be seen in Figure 3, the deviation of the head can be neglected after the cell number reaches 1.38 million. Therefore, a final cell number of 1,388,536 was utilized for the calculation.

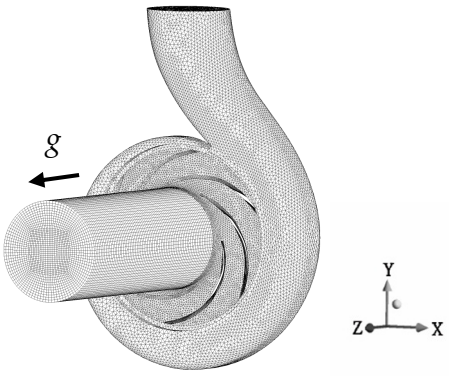

Figure 2. Computational domain and grids. g = gravitational acceleration.

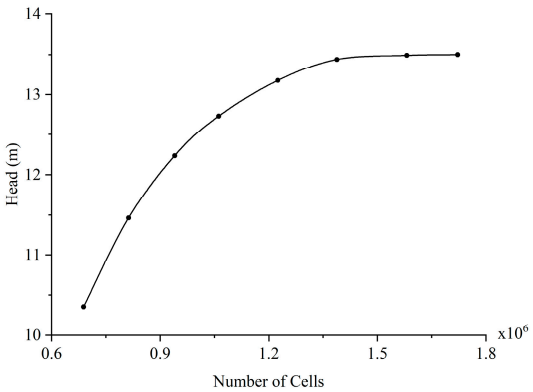

Figure 3. Grid independence analysis.

2.4. Material Properties and Interactions

The particle was assumed to be spherical in the simulation. The Hertz–Mindlin non-slip contact model was used for describing the particle–particle interactions and the Hertz–Mindlin with Archard wear model for particle–pump interactions, and the value wear constant K/H in Equation (1) was 1×10^{-12} [24]. The material properties of the pump and particles are shown in Table 1, and the coefficients of interactions are shown in Table 2.

Table 1. Material properties.

Material	Poisson's Ratio	Shear Modulus (mpa)	Density (kg/m^3)	Diameter (mm)	Volume Fraction At Pump Inlet (%)
pump	0.30	70.0×10^3	7800		
particle	0.40	21.3	1500	1.0–3.0	2

Table 2. Material interactions.

Interaction	Coefficient of Restitution	Coefficient of Static Friction	Coefficient of Rolling Friction
particle–particle	0.44	0.27	0.01
particle–pump	0.50	0.15	0.01

In the transient simulation, the impeller speed was assumed to be constant (n = 1450 r/min). In the initial state (t = 0), the velocity of the liquid phase was set to zero. When the computations were started, the solid particles were continuously released at the pump inlet, with the volume fraction of particles maintained at 2%, and the particle diameter varied randomly from 1.0 mm to 3.0 mm. The inlet boundary condition included the design flow rate of the pump, while the outlet boundary was given by the outlet pressure ($p = 1 \times 10^5$ Pa). The computations in Fluent were performed using the time step $\Delta t = 60/65nZ \approx 1 \times 10^{-4}$ s, which represents an impeller rotation of less than one degree. Therefore, the time step of 1×10^{-6} s was selected for the EDEM simulations to maintain the ratio of EDEM–Fluent simulation steps at 100:1.

3. Results and Analyses

3.1. Particle Distribution

For the purpose of studying the two-phase flow field in the centrifugal pump under different flow conditions, the calculations under $0.7Q_d$, $1.0Q_d$ and $1.3Q_d$ flow conditions were conducted under the premise of the constant volume fraction at the pump inlet. Figure 4 shows the calculated total volume of solid particles inside the pump V_P as a function of time t. As shown in the figure, after the initial state of particle release at t = 0, the total volume V_P increases with time t. When V_P approaches some values at a certain time, the centrifugal pump begins operating in a normal state. The time for reaching the normal state under $0.7Q_d$, $1.0Q_d$ and $1.3Q_d$ flow conditions is about 0.7 s, 0.5 s, and 0.3 s, respectively.

The distribution of particles when the pump operates normally is shown in Figure 5. As can be seen in the figure, as the flow rate Q increases, the particle trajectory in the impeller is biased toward the blade pressure side, and the trajectory downstream of the volute is gradually biased toward the gravity direction.

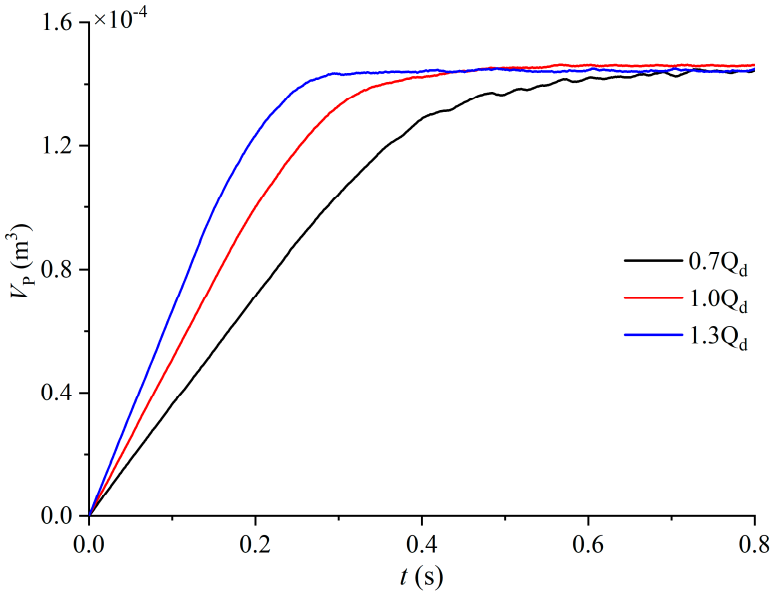

Figure 4. Variation of particle volume (V_P) inside the pump at different times (t) under different flow conditions. Q_d = capacity.

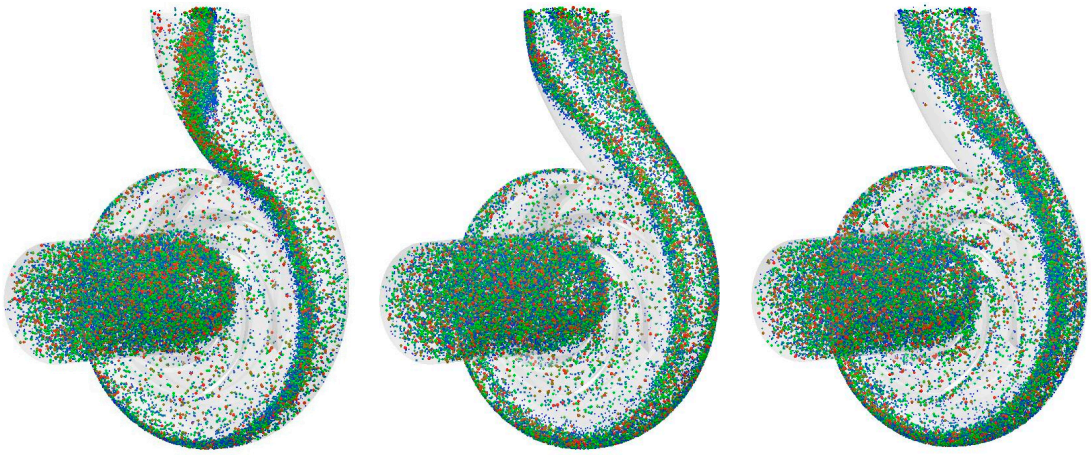

Figure 5. Particle distribution in the pump under different flow conditions. (**a**) $0.7Q_d$; (**b**) $1.0Q_d$; (**c**) $1.3Q_d$.

3.2. Wear Analysis of Flow Parts

Figure 6 illustrates the calculated distribution of wear per unit flow area h under three different flow conditions (t = 0.8 s). As the flow rate Q increases, the wear h in the pump also increases, which is consistent with the wear experiment results reported by Azimian et al. [16].

To study the wear distribution inside the pump, the calculation domain is divided into flow parts such as the leading edge of the impeller blade, blade tip, blade pressure side, blade suction side, impeller shroud, hub and volute. Figure 7 presents the wear h of each flow part in the pump under different flow conditions (t = 0.8 s). Figure 7a–d show that the wear in the impeller mainly occurs in the blade leading edge, the junction of the hub and the trailing part of the blade pressure side, and the junction of shroud and rear part of the blade suction side. These simulation results are consistent with the results of the paint wear experiment developed by Luo et al. [13] and the wear test rig by Tao et al. [17]. In addition, as the flow rate Q increases, the wear h of the blade pressure side and the impeller hub increases, the wear h of the shroud decreases, while that of the blade suction side does not change significantly. As shown in Figure 7e, the most serious wear region in the volute is the tongue

area. Because of the centrifugal force, the wear is more severe on the side of the hub in the upstream of the volute. In the downstream, as the kinetic energy of the particles decreases, the wear position is gradually biased toward the gravity direction.

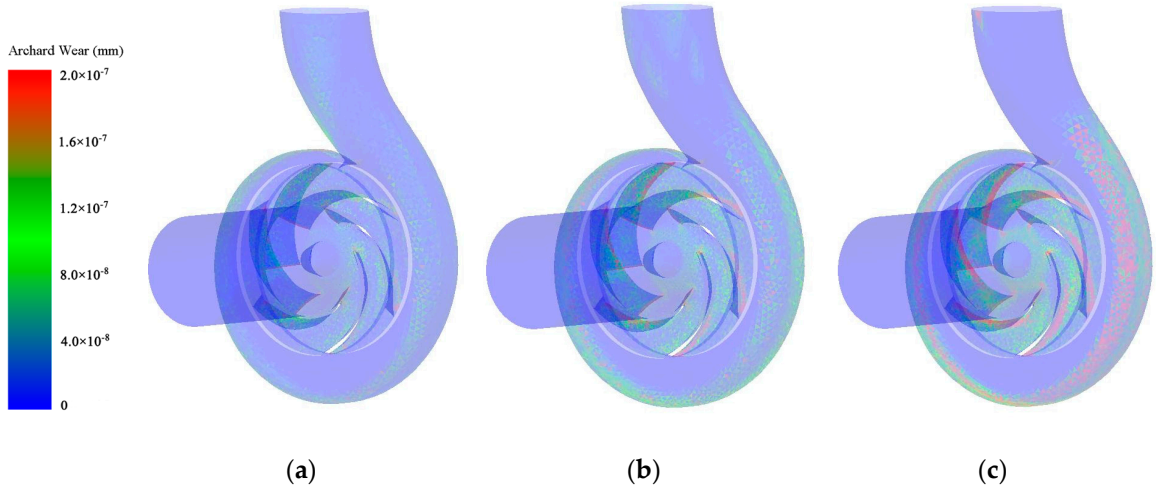

Figure 6. Wear distribution contour in the centrifugal pump at t = 0.8 s. (**a**) 0.7Q_d; (**b**) 1.0Q_d; (**c**) 1.3Q_d.

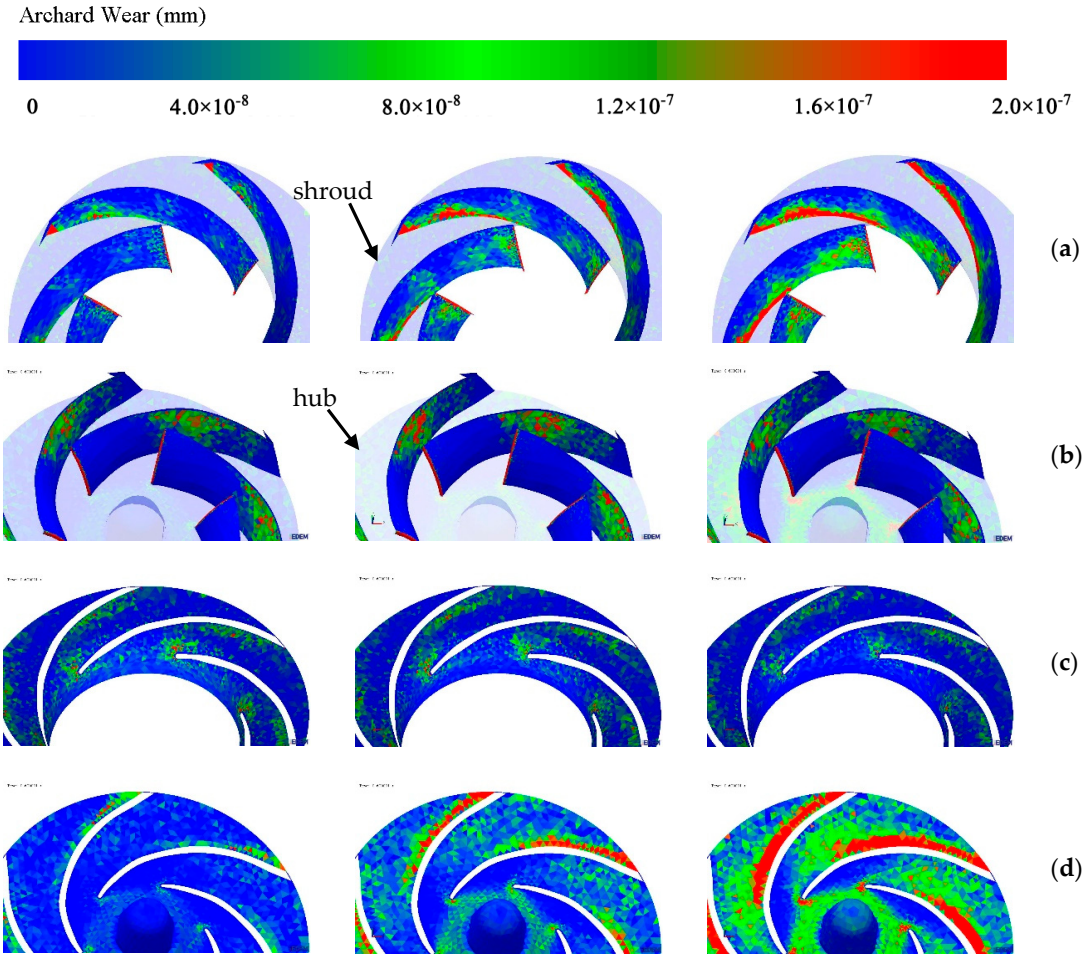

Figure 7. *Cont.*

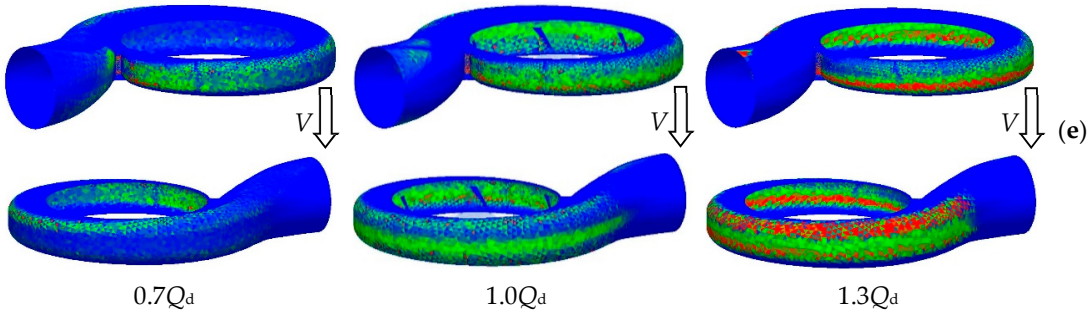

Figure 7. Wear distribution of pump parts at t = 0.8 s. (**a**) blade pressure side; (**b**) blade suction side; (**c**) impeller shroud; (**d**) impeller hub; (**e**) volute.

The wear volume W and the wear rate dW/dt of the flow parts in the pump under different flow rates Q as a function of time t are shown in Figure 8. As presented in Figure 8a, the wear volume of the volute is greater than that of the impeller. Under the 0.7Q_d flow condition, the order of wear volume of all flow parts in the impeller from high to low is as follows: impeller shroud, blade pressure side, blade suction side, impeller hub, blade leading edge, and blade tip. The order under the 1.0Q_d flow condition is: pressure side, hub, shroud, suction side, leading edge, and blade tip. The order under the 1.3Q_d flow condition is: pressure side, impeller hub, suction side, shroud, leading edge, and blade tip.

As shown in Figure 8b, the wear rate dW/dt of each flow part approaches steadily in a short period of time after particles begin entering the pump, and it is faster under higher flow conditions. The subsequent wear analysis would be carried out when the wear rate approached steady state.

The relationship between the total wear volume of the pump and the flow rate at t = 0.8 s was carried out through linear regression as seen in Figure 9. Thus, an equation can be conducted as below, which illustrates the approximately proportional relationship between the total wear volume and the flow rate:

$$W \propto Q^{1.0318} \tag{3}$$

Figure 10 shows the number of contacts N between the particles and the flow parts within five fundamental rotation periods of the impeller after the wear rate approached steady state (t = 0.0414 s). It can be seen that the number of contacts N is substantially proportional to the wear volume of the flow parts.

In order to obtain the quantitative wear, Figure 11 illustrates the relative wear amount W^* (t = 0.8 s) of each part of the pump under different flow conditions. The relative wear amount in Figure 11a is represented as the wear volume of the flow parts divided by the total wear volume of the pump. The relative wear amount in Figure 11b is represented as the wear volume of the flow parts divided by the total wear volume of the impeller. As can be seen from Figure 11a, the wear volume of the volute accounts for about 70% of the total wear volume of the pump, which is consistent with the results of the paint wear test by Roco [14]. The relative wear amount W^* of the impeller gradually increases from 25% to 30% as the flow rate Q increases. It is shown in Figure 11b that when the flow rate Q increases, the relative wear amount of the impeller hub increases significantly from 14% to 35%, followed by the blade pressure side, where W^* increases from 27% to 38%. Correspondingly, the relative wear amount of the impeller shroud is significantly reduced from 29% to 8%. Because the wear volume of the blade leading edge and the suction side does not change much, while the total wear volume of the pump increases, the W^* of these two parts shows a certain degree of decline. These results are basically consistent with the trends in the paint wear test conducted by Ahmad et al. [15].

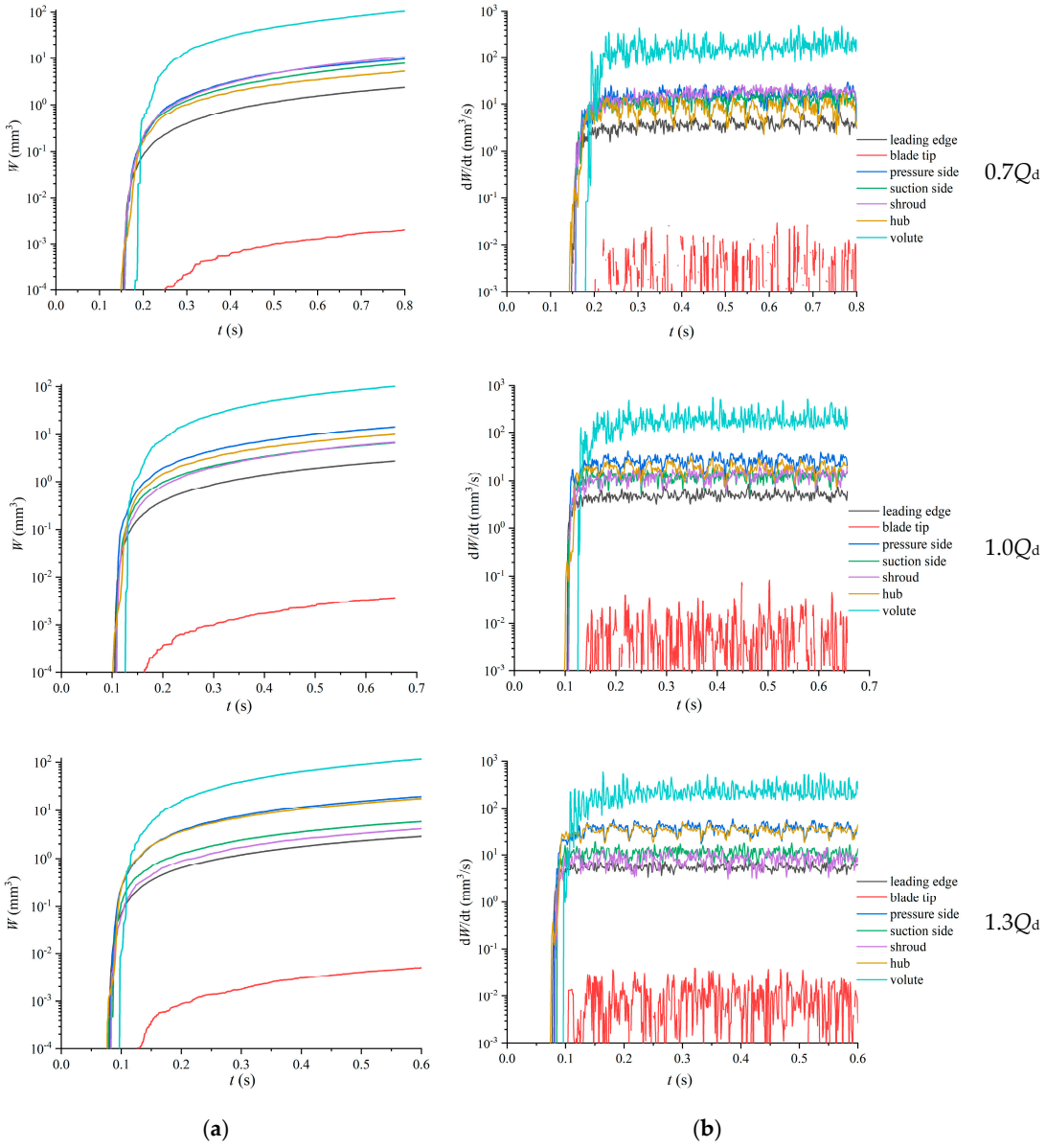

Figure 8. Wear volume and wear rate of flow parts as function of time. (**a**) Wear volume *W*; (**b**) Wear rate d*W*/dt.

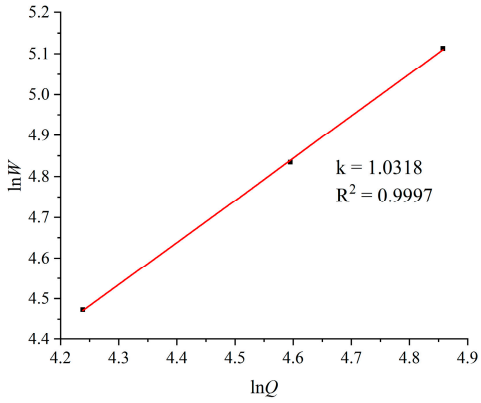

Figure 9. The effect of flow rate on the total wear volume of the pump. k = slope, R^2 = coefficient of determination.

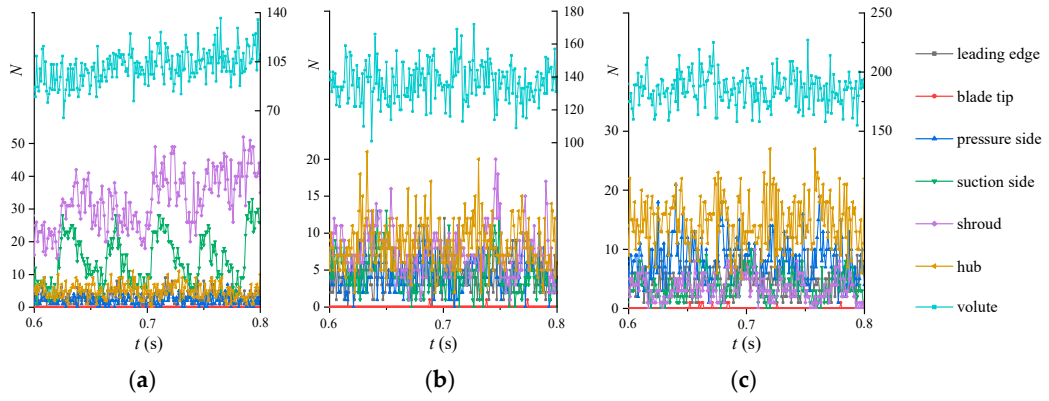

Figure 10. Numbers of contacts (N) of flow parts as function of time. (**a**) $0.7Q_d$; (**b**) $1.0Q_d$; (**c**) $1.3Q_d$.

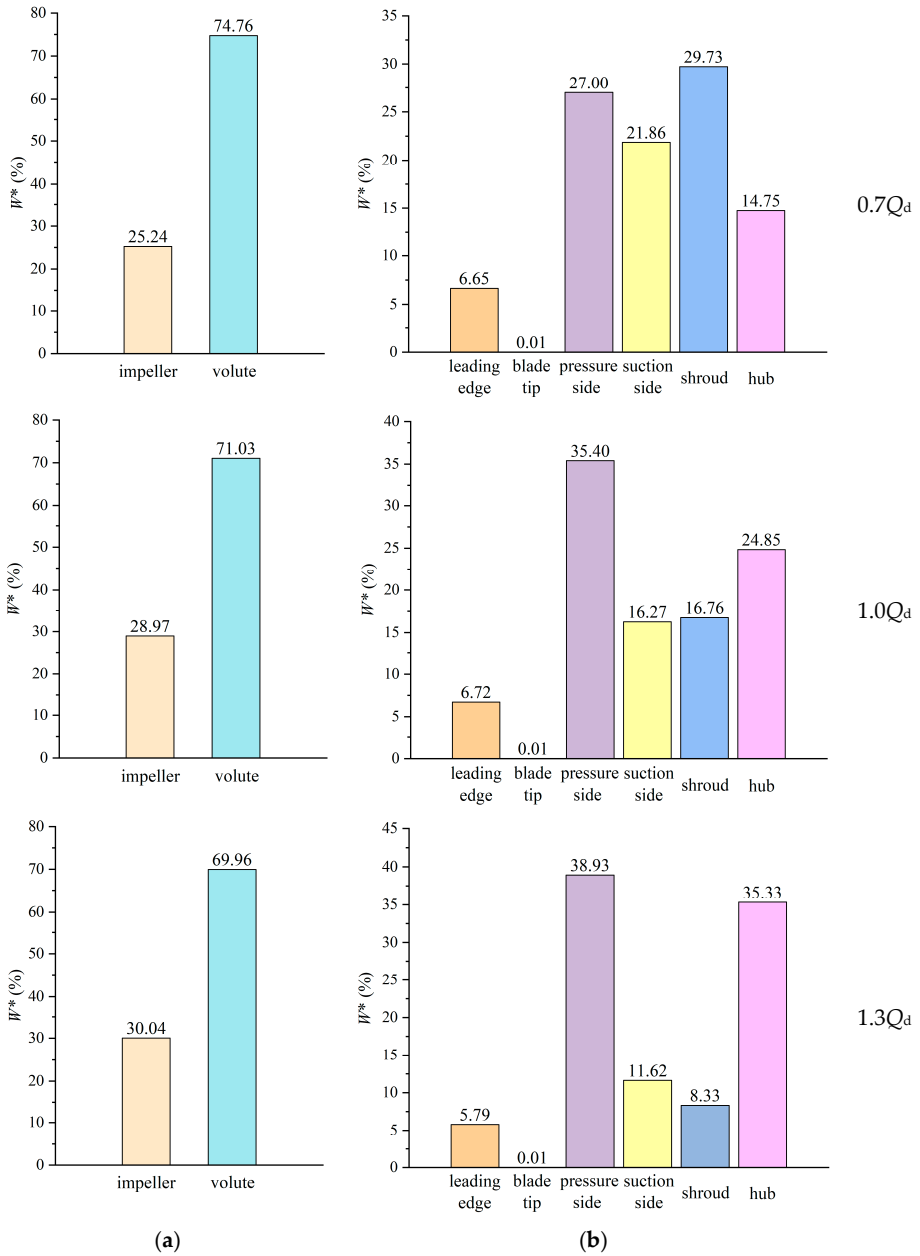

Figure 11. Relative wear amount (W^*) of flow parts at t = 0.8 s. (**a**) Pump; (**b**) Impeller.

4. Conclusions

By coupling the EDEM–Fluent method and introducing the wear model, the wear law of the centrifugal pump flow parts was developed and researched. Based on the calculation results, the following conclusions can be made:

(1) As the flow rate increases, the particle trajectory in the impeller is biased towards the blade pressure side; the kinetic energy of solid particles decreases along the volute casing, and its trajectory is gradually biased towards the gravity direction downstream.

(2) Under the flow conditions calculated, the wear volume of the volute accounts for approximately 70% of the total wear volume in the pump. The wear in the impeller mainly occurs in the blade leading edge, the junction of the hub and the trailing part of the blade pressure side, and the junction of the shroud and the rear part of the blade suction side. The number of contacts between the particles and the flow parts of the pump is substantially proportional to the wear volume of each part.

(3) The wear rate of each flow part approaches steady state within a short period of time, and it achieves steady state faster in higher flow conditions. Under the lower flow condition, the wear in the impeller shroud is relatively considerable. As the flow rate increases, the wear in the blade pressure side and the hub increases significantly.

Author Contributions: S.H., J.H. and J.G. conceived and designed the experiments; S.H. and J.H. performed the experiments; J.H. and J.G. analyzed the data; Y.M. contributed materials and analysis tools; S.H. and J.H. wrote the paper.

Funding: This research received no external funding.

Conflicts of Interest: The authors declare no conflict of interest.

References

1. Huang, S.; Su, X.H.; Qiu, G.Q. Transient numerical simulation for solid-liquid flow in a centrifugal pump by DEM-CFD coupling. *Eng. Appl. Comput. Fluid Mech.* **2015**, *9*, 411–418. [CrossRef]
2. Ning, C.; Wang, Y. Performance analysis on solid-liquid mixed flow in a centrifugal pump. *Iop Conf. Ser. Mater. Sci. Eng.* **2016**, *129*, 012062. [CrossRef]
3. Cheah, K.W.; Lee, T.S.; Winoto, S.H. Numerical study of inlet and impeller flow structures in centrifugal pump at design and off-design points. *Int. J. Fluid Mach. Syst.* **2011**, *4*, 25–32. [CrossRef]
4. Huang, S.J.; Shao, C.L. Solid-liquid two-phase flow characteristics in centrifugal pump with multi-component medium. *Trans. Chin. Soc. Agric. Eng.* **2016**, *32*, 77–84.
5. Torabi, R.; Nourbakhsh, S.A. The effect of viscosity on performance of a low specific speed centrifugal pump. *Int. J. Rotating Mach.* **2016**. [CrossRef]
6. Noon, A.A.; Kim, M.H. Erosion wear on centrifugal pump casing due to slurry flow. *Wear* **2016**, *364*, 103–111. [CrossRef]
7. Shen, Z.J.; Chu, W.L. Effect of particle parameters on erosion wear and performance of screw centrifugal pump. In Proceedings of the ASME International Mechanical Engineering Congress and Exposition, Pittsburgh, PA, USA, 9–15 November 2018; AMER SOC Mechanical Engineers: New York, NY, USA, 2019.
8. Peng, G.J.; Luo, Y.Y.; Wang, Z.W. Research on wear properties of centrifugal dredge pump based on liquid-solid two-phase fluid simulations. *Iop Conf. Ser. Mater. Sci. Eng.* **2015**, *72*. [CrossRef]
9. Singh, J.; Kumar, S.; Mohapatra, S.K. Study on role of particle shape in erosion wear of austenitic steel using image processing analysis technique. *Proc. Inst. Mech. Eng. Part. J. J. Eng. Tribol.* **2019**, *233*, 712–725. [CrossRef]
10. Lei, H.M.; Xiao, Y.X.; Chen, F.N.; Ahn, S.H.; Wang, Z.W.; Gui, Z.H.; Luo, Y.Y.; Zhao, X.R. Numerical simulation of solid-liquid two-phase flow in a centrifugal pump with different wear blades degree. *Iop Conf. Ser. Earth Environ. Sci.* **2018**, *163*. [CrossRef]
11. Pagalthivarthi, K.V.; Gupta, P.K.; Tyagi, V.; Navi, M.R. CFD prediction of erosion wear in centrifugal slurry pumps for dilute slurry flows. *J. Comput. Multiph. Flows.* **2011**, *3*, 225–245. [CrossRef]

12. Lai, F.; Zhu, X.Y.; Xu, X.; Li, G.J. Erosion wear and performance simulation of centrifugal pump for solid-liquid flow. In Proceedings of the ASME Power Conference, Lake Buena Vista, FL, USA, 24–28 June 2018; AMER SOC Mechanical Engineers: New York, NY, USA, 2018.
13. Luo, X.W.; Xu, H.Y.; Yan, Z.M.; Li, S.S. Analysis on the Wear Characteristic of ADI Blade for Slurry Pump. *J. Hydroelectr. Eng.* **2001**, *1*, 79–85.
14. Roco, M.C.; Addie, G.; Dennis, J.; Nair, P.; Bhra, F.; Snamprogetti, I. Modeling erosion wear in centrifugal slurry pumps. *Hydrotransport* **1984**, *9*, 291–316.
15. Ahmad, K.; Baker, R.C.; Goulas, A. Computation and experimental results of wear in a slurry pump impeller. *Proc. Inst. Mech. Eng. Part. C: J. Mech. Eng. Sci.* **1986**, *200*, 439–445. [CrossRef]
16. Azimian, M.; Bart, H.J. Erosion investigations by means of a centrifugal accelerator erosion tester. *Wear* **2015**, *328*, 249–256. [CrossRef]
17. Tao, Y.; Yuan, S.; Zhang, J.F.; Zhang, F.; Tao, J.P. Numerical simulation and test on impeller wear of slurry pump. *Trans. Chin. Soc. Agric. Eng.* **2014**, *30*, 63–69.
18. Zhu, Z.C.; Cui, B.; Li, Y. Experimental study on hydraulic performance and wear of double-channel pump delivering solid-liquid media. *J. Mech. Eng.* **2009**, *45*, 65–69. [CrossRef]
19. Tsuji, Y.; Kawaguchi, T.; Tanaka, T. Discrete particle simulation of two-dimensional fluidized bed. *Powder Technol.* **1993**, *77*, 79–87. [CrossRef]
20. Kafui, K.D.; Thornton, C.; Adams, M.J. Discrete particle-continuum fluid modelling of gas–solid fluidised beds. *Chem. Eng. Sci.* **2002**, *57*, 2395–2410. [CrossRef]
21. Finnie, I. Some observations on the erosion of ductile metals. *Wear* **1972**, *19*, 81–90. [CrossRef]
22. Grant, G.; Tabakoff, W. Erosion prediction in turbomachinery resulting from environmental solid particles. *J. Aircr.* **1975**, *12*, 471–478. [CrossRef]
23. Archard, J.F. Contact and rubbing of flat surfaces. *J. Appl. Phys.* **1953**, *24*, 981–988. [CrossRef]
24. Chen, G.; Schott, D.L.; Lodewijks, G. Sensitivity analysis of DEM prediction for sliding wear by single iron ore particle. *Eng. Comput.* **2017**, *34*, 2031–2053. [CrossRef]